

Effects of High-Power Ion Bernstein Waves on a Tokamak Plasma

M. Ono, P. Beiersdorfer, R. Bell, S. Bernabei, A. Cavallo, A. Chmyga,^(a) S. Cohen, P. Colestock, G. Gammel, G. J. Greene, J. Hosea, R. Kaita, I. Lehrman,^(b) G. Mazzitelli,^(c) E. Mazzucato, D. McNeill, K. Sato,^(d) J. Stevens, J. Timberlake, J. R. Wilson, and A. Wouters

Princeton Plasma Physics Laboratory, Princeton University, Princeton, New Jersey 08544

(Received 2 April 1987)

Effects of high-power ion-Bernstein-wave heating on the PLT tokamak plasmas have been investigated with up to 650 kW of rf power coupled to the plasma. A significant improvement in the deuterium particle confinement (as much as 300%) during high-power ion-Bernstein-wave heating has been observed. Associated with it, a longer injected-impurity-confinement time, reduced drift-wave turbulence activity, frequency shifts of drift-wave turbulence, and development of a large negative edge potential were observed. The ion heating efficiency, $\Delta T_i(0)\bar{n}_e/P_{rf} = 6 \times 10^{13}$ eV cm⁻³/kW, without high-energy tail ions, is relatively constant up to the maximum rf power.

PACS numbers: 52.50.Gj, 52.35.Hr

Plasma heating by directly launched ion Bernstein waves (IBWH) has been actively investigated in recent years.¹⁻⁸ As a result of their relatively short wavelength, the ion Bernstein waves can heat the bulk-ion distributions,¹ and the wave polarization and the relatively wide operating frequency range permit a flexible waveguide launcher design,^{9,10} attractive for the compact ignition device.¹¹ In previous lower-power tokamak IBWH experiments ($P_{rf} \approx 60$ – 150 kW), various interesting heating regimes were identified.^{2,3,12,13} These initial experiments demonstrated that IBWH can heat bulk ions even at relatively high harmonics of the ion cyclotron frequency without producing a significant high-energy ion-tail population. IBWH can also interact nonlinearly with subharmonics of the ion cyclotron frequencies, giving rise to new heating scenarios.^{2,6,7,13}

In this paper, we report results of the PLT experiments where the plasma transport and microturbulence activities were significantly altered as a result of the application of high-power IBWH ($P_{rf} \gtrsim P_{OH}$). The corresponding heating and energy confinement behavior is also discussed.

In order to excite preferentially the ion Bernstein wave, a B_θ - E_z type loop coupler was used.² The high-power IBWH antenna is a 60-cm-long and 5-cm-wide single-loop antenna which is shielded from the plasma by two layers of stainless-steel Faraday shields. The plasma loading for this antenna was $\approx 2 \Omega$, resulting in (80–90)% coupling of the applied rf power to the plasma.¹⁴

IBWH at high power levels was performed in PLT circular limiter discharges with major and minor radii of 132 and 39 cm. With two IBWH antennas, up to 650 kW of rf power was coupled to the plasma. The ^3He and $\frac{3}{2} \Omega_D$ heating regimes were investigated with use of the PLT 30-MHz transmitters. Typical heating results are shown in Fig. 1(a), where a time evolution of the ion temperature is shown for $\frac{3}{2} \Omega_D$ heating at the 500-kW

level in a deuterium plasma with $\bar{n}_e = 3 \times 10^{13}$ cm⁻³. Three T_i diagnostic techniques, Doppler broadening (TiXXI), charge exchange (Cx), and neutron emission, are in good general agreement within the uncertainties of each diagnostic. The charge-exchange velocity distribution is Maxwellian without any high-energy tail ions up

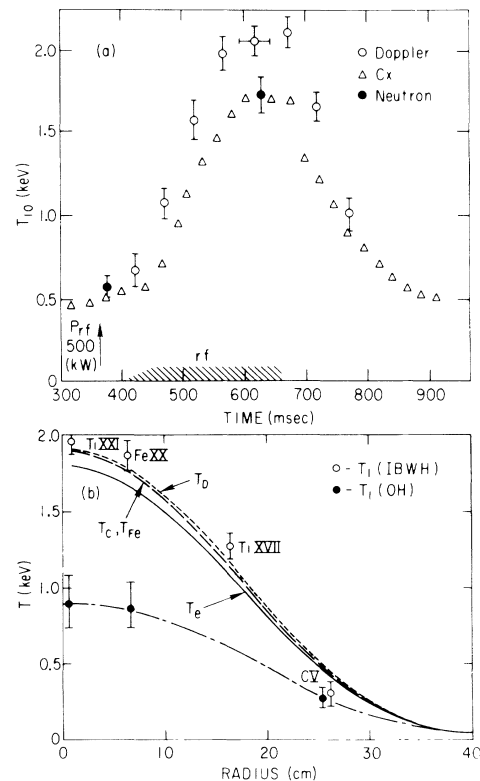


FIG. 1. (a) A typical time evolution of ion temperature. $P_{rf} = 500$ kW, $F = 30$ MHz, $B_0 = 29$ kG, $\frac{3}{2} \Omega_D$, $I_p = 500$ kA, $P_{OH} = 550$ kW, and $\bar{n}_e = 3.0 \times 10^{13}$ cm⁻³. (b) Temperature profiles at $t = 600$ msec.

to the highest-power level. The ion-temperature profile as measured by the Doppler broadening of various ion lines is centrally peaked [Fig. 1(b)]. In the 500–600-kW range, the central Doppler ion temperature reaches ≈ 2 keV, which exceeds the central television Thomson-scattering electron temperature. The time evolution of the plasma density is shown in Fig. 2(a). The dashed curves are that of an Ohmic case where the gas feed is programmed to yield a similar density evolution.

During IBWH, the particle confinement shows a significant improvement.⁴ A clear example is shown in Fig. 2(a), where the plasma density increases by more than a factor of 3. This occurs without active gas puffing and without increasing particle recycling, as indicated by a drop in the D_α emission. As shown in Fig. 2(b), the D_α emission near the antenna-limiter region (the main recycling region) during IBWH (solid curve) is significantly less than that in the programmed OH (dashed curve) case. This density rise during IBWH does not correlate with the impurity influx measured by various spectroscopic instruments, a bremsstrahlung-based Z meter, and a scanning bolometer. This behavior can be seen in Fig. 2(a) where the time evolution of average Z_{eff} , $\langle Z_{\text{eff}} \rangle \propto I_{\text{brem}} T_e^{1/2} n_e^{-2}$, where I_{brem} is the bremsstrahlung radiation intensity, is plotted. Also, the large increase in neutron level (a factor of 500) shows that the incremental density is due mainly to deuterium. The density profiles during IBWH are peaked, similar to the simulated Ohmic case.

Associated with this improvement in the particle confinement, a number of interesting phenomena were

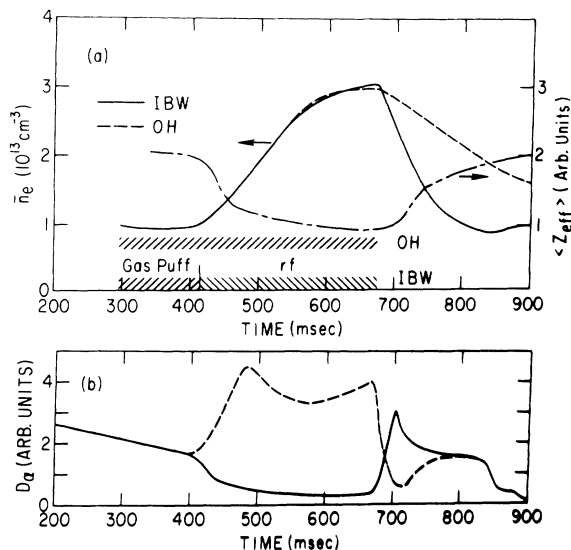


FIG. 2. (a) Density time evolution for IBWH case (solid curve) shown in Fig. 1 and Ohmic case (dashed curve), in which the gas puffing was used to simulate the density rise of the IBWH case. $\langle Z_{\text{eff}} \rangle$ evolution during IBWH is shown by the broken curve. (b) Time evolution of D_α emission for IBWH and Ohmic cases taken near the antenna-limiter region.

observed. During IBWH, the low-energy neutral flux levels (at energies less than 1 keV) decrease significantly.⁷ This drop may be related to the drop in the D_α emission. In order to understand further the particle transport processes during IBWH, a laser blowoff impurity injector was used to inject a trace amount of selenium. The decay time of the Se XXV radiation increases by a factor of 2 from the Ohmic level (from 50 to 100 msec). Since during the observation time, the central electron density and temperature are nearly constant for both cases, the selenium-line behavior gives an indication of the central selenium confinement. Similar behavior was observed with a helium gas puff. With injection of a given amount of helium with a preprogrammed fast gas valve, the net density rise during IBWH is at least twice the level of the no rf case, again suggesting an improvement in the particle confinement time. The similar confinement behavior for low- Z ions (hydrogen and helium) and high- Z ions (selenium) suggests nonneoclassical particle diffusion behavior.¹⁵

Another striking effect of IBWH is in the change of the low-frequency turbulence activity in the plasma. A microwave scattering system¹⁶ was used to investigate the turbulence in a half-radius region between the $q=1$ and $q=3$ surfaces, $r=25 \pm 10$ cm. It is generally believed that the low-frequency turbulence activity in this region plays an important role in anomalous transport processes in tokamak plasmas.¹⁷ In Fig. 3(a), the time

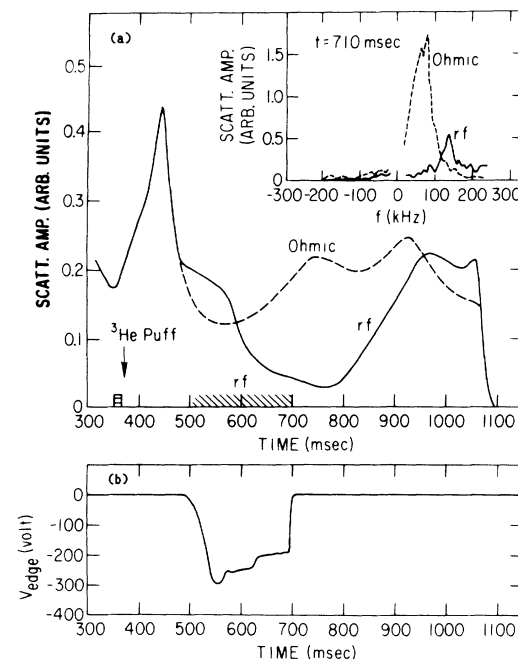


FIG. 3. (a) Time evolution of low-frequency turbulence level at 100 kHz for the two cases. $k(\text{scatt})=6-8 \text{ cm}^{-1}$ at $r=25 \pm 10$ cm. Inset: Frequency spectrum at $t=710$ msec for the two cases. (b) Time evolution of the plasma edge floating potential.

evolutions of the scattering signals at 100 kHz for both the IBWH and simulated Ohmic cases are shown. In this case, the scattered wave number is $6\text{--}8\text{ cm}^{-1}$. One can see a significant drop in the turbulence level during IBWH as compared to the simulated Ohmic case. In the inset, the frequency spectrum in each case is shown immediately after the end of rf ($t = 710\text{ msec}$). A frequency shift along with the amplitude reduction occurs during IBWH. Since the plasma density and electron temperature profiles are similar in both cases, one can rule out the possibility of a change in the scattering volume or the diamagnetic drift velocity. From the frequency shift, one can infer a net increase of the poloidal rotational velocity of approximately $5 \times 10^4\text{ cm/sec}$ in the electron diamagnetic drift direction. This drift velocity would correspond to an electric field of 15 V/cm in the radially inward direction. It should be noted here that this clear reduction in the drift-wave activity correlates well with a longer impurity particle confinement time. Measurements with an rf-shielded Langmuir probe in the plasma edge have shown the development, during IBWH, of a large floating potential which is negative with respect to the chamber wall [Fig. 3(b)]. This observation is again correlated with the appearance of a frequency shift in the turbulence spectrum. These observations may be related to the results of recent limiter-bias experiments, where negative bias has produced some im-

provement in particle confinement with a corresponding reduction in the edge low-frequency turbulence activity.¹⁸ Reduced turbulence activity was also observed during the *H*-mode phase of neutral-beam-heated PDX plasmas where the particle confinement showed an improvement.¹⁹

Plasma energy confinement during IBWH is of interest because of its bulk-ion heating properties. The ion heating efficiency as shown in Fig. 4(a) is nearly constant up to a 650-kW level, with a heating quality factor of $\Delta T_i(0)\bar{n}_e/P_{rf} = (6\text{--}7) \times 10^{13}\text{ eV cm}^{-3}/\text{kW}$ which is comparable to the best PLT ion cyclotron-resonance heating efficiency.²⁰ It is interesting to note that both ^3He and $\frac{3}{2}\Omega_D$ heating have similar heating efficiencies. The toroidal magnetic field for $\frac{3}{2}\Omega_D$ heating is about 10% lower than the ^3He case and the $\frac{3}{2}\Omega_D$ regime, of course, requires no ^3He injection. The ion heating efficiency decreases significantly when the resonance layer is moved outside of the $q=1$ surface, $r \approx 15\text{ cm}$. In Fig. 1(b), the calculated ion-temperature profiles, on the assumption of an Ohmic ion-energy diffusion coefficient, are plotted as dashed curves and agree quite well with the measured profile. This provides an indication that no significant ion-transport deterioration occurred during IBWH.¹³ However, the global energy confinement shows a gradual degradation of confinement time with increased rf power as shown in Fig. 4(b). At 650 kW, the confinement time is about 40 msec at $\bar{n}_e = 4.5 \times 10^{13}\text{ cm}^{-3}$, which is significantly below the Ohmic value of 50–55 msec, but appears to be higher than the *L*-mode scaling time of $\approx 33\text{ msec}$.²¹ The IBWH confinement time actually increases with the plasma density, similar to the results on PLT with fast-wave ion-cyclotron-range-of-frequencies heating,²² whereas neutral-beam *L*-mode scaling tends to be relatively constant with density. The deviation from Ohmic confinement can be attributed to an increase in the electron-loss channel, which is mainly due to the increased radiation loss. The radiation profile during IBWH as measured by a scanning bolometer shows a more centrally peaked profile, with the total radiated power increasing by a factor of 3. However, the electron diffusivity, which takes this radiation loss into account, remains Ohmic-like.

To investigate the scaling of energy confinement with plasma current, the current was varied between 200 kA ($q_{\text{edge}} = 10$) to 630 kA ($q_{\text{edge}} = 3$) with a constant rf power level of 250 kW. The PLT discharges in this current range exhibit sawtoothing activities and the radiation loss is relatively small for this rf power level. We find that for a given rf power, the ion-temperature increase remains constant down to the lowest current of 200 kA. The normalized confinement time, τ_E/\bar{n}_e , also remains relatively constant. This behavior may be due to the bulk-ion heating characteristic of IBWH that fast ion losses are negligible, even for the low-current case.

In conclusion, with application of high-power IBWH

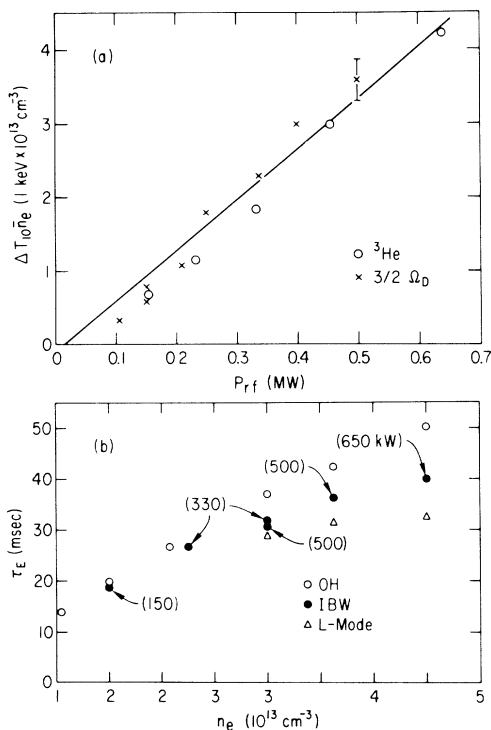


FIG. 4. (a) Ion heating as a function of rf power for ^3He -minority regimes. (b) Global energy confinement time as a function of the plasma line-averaged density.

($P_{rf} \gtrsim P_{OH}$), significant improvement in the deuterium particle confinement and reduction in the microturbulence activity were observed. Correlated with this behavior, longer confinement time of injected selenium and helium and development of a radially inward electric field and of a large negative edge floating potential were observed. The ion heating produced very few tail ions and remained efficient up to the highest power level ($P_{rf} \approx 650$ kW). The global plasma energy-confinement time at the highest power levels showed some degradation from the Ohmic level, which was attributed to an increase in radiative losses. The ion heating and the energy confinement remained relatively constant as the plasma current varied. It is interesting to note that over all, IBWH-produced plasmas have many similarities with H -mode plasmas although the IBWH-produced plasmas show more peaked density profiles, an indication of the particle-transport improvement in the inner region of the plasma.

The authors appreciated the support and encouragement given to the experiment by K. Bol, T. H. Stix, P. Rutherford, and H. Furth. One of the authors (M.O.) also appreciated discussions with Dr. M. Okamoto concerning plasma transport. This work was supported by U.S. Department of Energy Contract No. DE-AC02-76-CHO-3073.

(a)Present address: Kharkov Physico-Technical Institute, Kharkov, U.S.S.R.

(b)Present address: Grumann Space Systems, Plainsboro, NJ 08536.

(c)Present address: Associazione EURATOM-ENEA, Frascati, Italy.

(d)Present address: Institute of Plasma Physics, Nagoya,

Japan.

¹M. Ono, G. A. Wurden, and K. L. Wong, *Phys. Rev. Lett.* **52**, 37 (1984).

²M. Ono *et al.*, *Phys. Rev. Lett.* **54**, 2339 (1985).

³T. Watari, in *Proceedings of the Course and Workshop on Applications of rf Waves to Tokamak Plasmas, Varenna, Italy, 1985*, edited by S. Bernabei, U. Gasparino, and E. Sindoni (International School of Physics "Piero Caldirola," Milan, 1985).

⁴J. C. Hosea *et al.*, *Plasma Phys. Controlled Fusion* **28**, 1241 (1986).

⁵J. R. Wilson *et al.*, *J. Nucl. Mater.* **145-146**, 616 (1987).

⁶H. Abe *et al.*, *Phys. Rev. Lett.* **53**, 1153 (1984).

⁷M. Porkolab *et al.*, *Phys. Rev. Lett.* **54**, 434 (1985).

⁸M. Porkolab *et al.*, in *Proceedings of the Eleventh International Conference on Plasma Physics and Controlled Nuclear Fusion Research, Kyoto, Japan, 1986* (IAEA, Vienna, to be published), Paper No. F-II-2.

⁹S. Puri, *Phys. Fluids* **22**, 1716 (1979).

¹⁰M. Ono *et al.*, in *Proceedings of the Eighth International Conference on Plasma Physics and Controlled Nuclear Fusion Research, Brussels, 1980* (IAEA, Vienna, 1981), Paper No. T-I-2(B).

¹¹J. Schmidt *et al.*, in Ref. 8, Paper No. H-I-2.

¹²J. R. Wilson, in *Radiofrequency Plasma Heating—1985*, edited by D. G. Swanson, AIP Conference Proceedings No. 129 (American Institute of Physics, New York, 1985), p. 8.

¹³M. Ono, in Ref. 12, p. 83.

¹⁴G. J. Greene *et al.*, *Bull. Am. Phys. Soc.* **31**, 1467 (1986).

¹⁵R. C. Isler, *Nucl. Fusion* **24**, 1599 (1984).

¹⁶E. Mazzucato, *Phys. Fluids* **21**, 1063 (1978), and *Phys. Rev. Lett.* **48**, 1828 (1982).

¹⁷P. C. Liewer, *Nucl. Fusion* **25**, 543 (1985).

¹⁸P. E. Phillips *et al.*, *J. Nucl. Mater.* **145-146**, 807 (1987).

¹⁹T. Crowley and E. Mazzucato, *Nucl. Fusion* **25**, 507 (1985).

²⁰J. Hosea *et al.*, in Ref. 10, Paper No. D-5-1.

²¹S. M. Kaye, *Phys. Fluids* **28**, 2327 (1985).

²²P. Colestock *et al.*, *Bull. Am. Phys. Soc.* **30**, 1445 (1985).